

Cite this: *Dalton Trans.*, 2021, **50**, 3269Received 28th December 2020,  
Accepted 29th January 2021

DOI: 10.1039/d0dt04401f

rsc.li/dalton

# Ruthenium complexes of phosphine–amide based ligands as efficient catalysts for transfer hydrogenation reactions†

Samanta Yadav, Paranthaman Vijayan, Sunil Yadav and Rajeev Gupta \*

This work presents three mononuclear Ru(II) complexes of tridentate phosphine–carboxamide based ligands providing a NNP coordination environment. The octahedral Ru(II) ion shows additional coordination with co-ligands; CO, Cl and CH<sub>3</sub>OH. All three Ru(II) complexes were thoroughly characterized including their crystal structures. These Ru(II) complexes were utilized as catalysts for the transfer hydrogenation of assorted carbonyl compounds, including some challenging biologically relevant substrates, using isopropanol as the hydrogen source. The binding studies illustrated the coordination of the isopropoxide ion by replacing a Ru-ligated chloride ion followed by the generation of the Ru–H intermediate that was isolated and characterized and was found to be involved in the catalysis.

## Introduction

The hydrogenation of organic compounds is one of the most fundamental transformations in organic chemistry.<sup>1–3</sup> The reduction of a multiple bond can be achieved conventionally by using hydrogen gas; however, an attractive alternative is the use of an organic compound as a hydrogen donor, the so called transfer hydrogenation (TH).<sup>4,5</sup> TH is a convenient method as it requires neither hazardous high-pressurized hydrogen gas nor a sophisticated experimental setup.<sup>6</sup> Furthermore, many inexpensive hydrogen donors are readily available and easy to handle.<sup>7–9</sup> In the TH of carbonyl compounds, many successful catalysts are based on transition metals as they exhibit excellent activity and selectivity both under the moderate temperature and reaction conditions.<sup>10</sup> The emergence of late transition-metal based catalysts, particularly involving metals of groups 8, 9, 10 and 11, has resulted in many noteworthy catalysts.<sup>11</sup> In particular, N-heterocyclic carbene (NHC) compounds of ruthenium and rhodium have been used as successful catalysts in the TH of carbonyl compounds.<sup>12</sup> Recently, Ding and co-workers<sup>13</sup> have shown that the Ir(III) complex of a benzothiazole-based ligand can be used for the hydrogenation of acetophenone. Shvo and

co-workers<sup>14</sup> have successfully developed an effective cyclopentadienyl ruthenium catalyst for the reduction of ketones *via* TH in a concerted pathway. The notable work of Henbest and Mitchell and co-workers<sup>15</sup> has illustrated the use of an [Ir–H] complex for the hydrogenation of cyclohexanones and  $\alpha,\beta$ -unsaturated ketones to their corresponding alcohols using isopropanol as the hydrogen source. Sasson and Blum<sup>16</sup> have shown that [RuCl<sub>2</sub>(PPh<sub>3</sub>)<sub>3</sub>] acts as an active catalyst for the biphasic TH of acetophenone with isopropanol. Chowdhury and Bäckvall<sup>17</sup> have concluded that the [RuCl<sub>2</sub>(PPh<sub>3</sub>)<sub>3</sub>] catalyzed TH reaction can be accelerated 10<sup>3</sup>–10<sup>4</sup> times upon adding a strong base.

Although many reagents such as alcohols,<sup>18</sup> formic acid–triethylamine<sup>19</sup> and sodium formate<sup>20</sup> have been used as H<sub>2</sub>-alternative hydrogenation agents of carbonyl compounds for the synthesis of secondary alcohols, isopropanol (2-propanol) has been found to be the best.<sup>21</sup> 2-Propanol is not only a safe, cheap, non-toxic and environment friendly hydrogen donor, but also a convenient solvent of choice thus eliminating the requirement of a separate solvent.<sup>21</sup> The presence of a strong base such as NaOH, KOH or KO<sup>t</sup>Bu is usually necessary for most TH reactions while using 2-propanol.<sup>22</sup> Primary alcohols, such as methanol and ethanol, are generally not employed as hydrogen donors because of their unfavourable redox potential.<sup>23</sup>

In this work, we report Ru(II) complexes supported with phosphine–carboxamide based tridentate ligands also containing other co-ligands (CO, Cl and CH<sub>3</sub>OH). The chelating ligands coordinate the Ru(II) ion as NNP donors. These Ru(II) complexes have been utilized for the transfer hydrogenation of assorted carbonyl compounds, including some biologically relevant substrates, using isopropanol as the hydrogen source. The mechan-

Department of Chemistry, University of Delhi, Delhi – 110 007, India.

E-mail: rgupta@chemistry.du.ac.in; http://people.du.ac.in/~rgupta/

† Electronic supplementary information (ESI) available: Figures for FTIR, UV/Vis, NMR and mass spectra; cyclic voltammetry; spectral titrations including fittings; gas chromatograms and tables for X-ray data collection and bonding parameters. CCDC 1993891–1993893. For ESI and crystallographic data in CIF or other electronic format see DOI: 10.1039/d0dt04401f

istic investigations including binding studies illustrated the coordination of the isopropoxide ion to the Ru(II) center before the generation of the Ru–H intermediate that was isolated and characterized and was found to participate in the TH catalysis.

## Results and discussion

### Synthesis and characterization of Ru(II) complexes

This work presents three novel closely related phosphine–carboxamide ligands; *N*-(2-(diphenylphosphanyl)phenyl)pyridine-1-carboxamide (HL<sup>1</sup>), *N*-(2-(diphenylphosphanyl)phenyl)isoquinoline-1-carboxamide (HL<sup>2</sup>) and *N*-(2-(diphenylphosphanyl)phenyl)quinoline-2-carboxamide (HL<sup>3</sup>). These ligands were synthesized by the coupling of 2-aminodiphenylphosphine with the respective carboxylic acid in pyridine using P(OPh)<sub>3</sub>. All three ligands were obtained in high yield and thus the present synthetic method is not only convenient but also high-yielding when compared to the methods reported in the literature.<sup>24</sup> These ligands were characterized by FTIR, <sup>1</sup>H, <sup>13</sup>C and <sup>31</sup>P NMR spectra as well as ESI<sup>+</sup> mass spectra (Fig. S1–S15, ESI<sup>†</sup>). The Ru(II) complexes 1–3 were respectively synthesized by refluxing ligands HL<sup>1</sup>–HL<sup>3</sup> with [Ru(CO)<sub>2</sub>(Cl)<sub>2</sub>]<sub>n</sub> in MeOH (Scheme 1). In the resultant Ru(II) complexes, all three ligands acted as tridentate ones and coordinated *via* anionic N<sub>amide</sub>, neutral P<sub>diphenylphosphine</sub> and neutral N<sub>pyridine</sub>/N<sub>quinoline</sub>/N<sub>isoquinoline</sub> sites *via* two five-membered chelate rings.

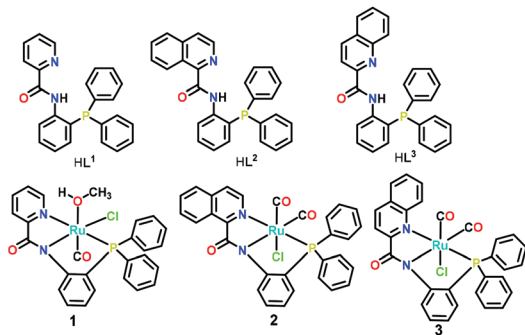
All three Ru(II) complexes were non-electrolytic in nature as confirmed by their molar conductivity.<sup>25a</sup> The FTIR spectra of the Ru(II) complexes (Fig. S16–S18, ESI<sup>†</sup>) showed the disappearance of the N–H stretches (at 3271, 3226 and 3235 cm<sup>-1</sup> for HL<sup>1</sup>, HL<sup>2</sup> and HL<sup>3</sup>, respectively) and bathochromically shifted C=O<sub>amide</sub> bands (1615–1627 cm<sup>-1</sup>) when compared to those of the corresponding ligands (1678–1688 cm<sup>-1</sup>).<sup>25b,26</sup> Both these features asserted the involvement of the deprotonated form of the amide group (N<sub>amidate</sub>) in the resulting Ru(II) complexes.<sup>25b,26</sup> The FTIR spectrum of complex 1 showed a single peak for the terminally coordinated carbonyl group at 1939 cm<sup>-1</sup> whereas complexes 2 and 3 exhibited two stretches at 1984/2049 and 1974/2043 cm<sup>-1</sup>, respectively, due to the presence of two CO groups.<sup>25b,26</sup> Both quinoline and isoquinoline

rings are more π-electron deficient heterocycles when compared to a pyridine ring.<sup>27</sup> As a result, the Ru(II) ion is more electron-deficient in complexes 2 and 3 and such a situation resulted in the coordination of two CO groups as better co-ligands. Such a fact is clearly demonstrated in the FTIR spectra wherein ν<sub>CO</sub> bands for 2 and 3 were observed at higher energy when compared to those for 1. This was due to an increase in the electron donation ability of a pyridine ring in 1 as compared to that of the quinoline and isoquinoline rings in 2 and 3.

The UV-visible spectra of complexes 1–3 in DMF displayed λ<sub>max</sub> between 360 and 430 nm which are tentatively assigned to ligand-to-metal charge transfer (LMCT) transitions (Fig. S19, ESI<sup>†</sup>).<sup>26</sup> All Ru(II) complexes have been thoroughly characterized using <sup>1</sup>H, <sup>13</sup>C and <sup>31</sup>P NMR spectra (Fig. S20–S28, ESI<sup>†</sup>). The proton NMR spectrum of complex 1 showed a signal corresponding to the CH<sub>3</sub> group of the coordinated methanol at 3.5 ppm (Fig. S20, ESI<sup>†</sup>). The <sup>13</sup>C NMR spectra of complexes 1–3 showed C≡O resonances between 196.6 and 204.2 ppm which are comparable to those of other Ru(II) carbonyl complexes (Fig. S23–S25, ESI<sup>†</sup>).<sup>26</sup> The <sup>31</sup>P NMR spectra of complexes 1–3 displayed one sharp singlet between 49.8–50.5 ppm for the phosphine group (Fig. S26–S28, ESI<sup>†</sup>). Such <sup>31</sup>P signals are considerably downfield shifted when compared to those of the ligands (–19.21, –17.96 and –18.58 ppm for HL<sup>1</sup>, HL<sup>2</sup> and HL<sup>3</sup>, respectively) asserting the involvement of the phosphine group in the coordination to the Ru(II) center.<sup>26</sup> The ESI<sup>+</sup> mass spectra of complexes 1–3 showed the most abundant peak assigned to the [M + H]<sup>+</sup> species (Fig. S29–S34, ESI<sup>†</sup>). In all cases, the observed isotopic distribution patterns matched perfectly the simulation patterns.

### Crystal structures

The solid-state molecular structures of all three Ru(II) complexes were determined by single crystal X-ray diffraction analyses (Fig. 1 and Tables S1 and S2, ESI<sup>†</sup>). The crystal structures displayed the presence of a tridentate chelating ligand coordinating in a NNP fashion in addition to assorted co-ligands (Cl, CO and CH<sub>3</sub>OH). Notably, both complexes 2 and 3 showed a very similar coordination environment around the Ru(II) center with a NNP ligand, one chloride anion and two CO ligands. In contrast, complex 1 showed a NNP ligand in addition to a chloride anion and a methanol molecule (Ru–O<sub>MeOH</sub> = 2.183 Å). For all three complexes, the Ru–Cl bond distance



**Scheme 1** Ligands HL<sup>1</sup>, HL<sup>2</sup>, and HL<sup>3</sup> and their Ru(II) complexes 1–3 discussed in this work.

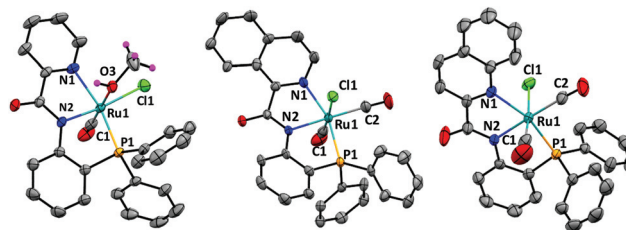


**Fig. 1** Thermal ellipsoidal representations (with 50% probability) of ruthenium complexes 1–3. Only methanol hydrogen atoms (in pink colour) are shown in complex 1 for clarity.

varied between 2.408 and 2.422 Å.<sup>26</sup> The crystal structures revealed that the Ru(II) ion is present in a nearly octahedral environment in all three complexes.<sup>26</sup> Despite the anionic  $\sigma$ -donation from the deprotonated  $N_{\text{amide}}$  group to the Ru(II) ion, the Ru– $N_{\text{amide}}$  bond distances (2.068, 2.073 and 2.088 Å for complexes 1–3, respectively) were comparable to the Ru– $N_{\text{pyridine}}/N_{\text{quinoline}}/N_{\text{isoquinoline}}$  bond distances (2.068–2.088 Å).<sup>28</sup> These complexes showed Ru–CO bond distances between 1.811 and 1.895 Å.<sup>26,29</sup> As expected, two phenyl rings of the diphenylphosphine moiety were located above and below the basal plane maintaining a tetrahedral geometry around the phosphorus atom.<sup>30</sup>

All three Ru(II) complexes exhibited several notable features that suggested their potential applications in catalysis. All three complexes displayed the presence of labile co-ligands, chloride anions, in all three cases in addition to a methanol in complex 1. Such a fact suggests that a suitable substrate and/or reagent may replace such labile ligand(s) creating interesting catalysis opportunities.<sup>31</sup> In all three complexes, NNP-based coordination constituted one anionic and two neutral donors. Such a situation provides a balanced electron donation at the ruthenium center and is likely to stabilize variable oxidation states of the ruthenium ion (*cf.* electrochemistry).<sup>26,32</sup> The presence of the diphenylphosphine group creates steric hindrance that would allow a substrate to only approach from the opposite side. The presence of pyridine, quinoline and isoquinoline rings is likely to subtly alter the electron density at the ruthenium center and may also have some effects on the catalysis.

### Electrochemistry

All three complexes were subjected to cyclic voltammetric (CV) studies in CH<sub>3</sub>OH (Fig. S35, ESI†). Complexes 1 and 2 exhibited an irreversible Ru<sup>3+</sup>/Ru<sup>2+</sup> redox couple with  $E_{\text{pa}}$  of 1.12 and 1.08 V versus the Fc<sup>+</sup>/Fc couple, respectively.<sup>26,32</sup> Complex 3, on the other hand, showed a nearly reversible response with the  $E_{\frac{1}{2}}$  value of 1.32 V ( $\Delta E_{\text{p}} = 90$  mV). All three complexes also displayed highly negative but reversible to quasi-reversible responses for the Ru<sup>2+</sup>/Ru<sup>+</sup> couple with  $E_{\frac{1}{2}}$  values of –1.72 V ( $\Delta E_{\text{p}} = 180$  mV), –1.48 V ( $\Delta E_{\text{p}} = 80$  mV) and –1.61 V ( $\Delta E_{\text{p}} = 100$  mV), respectively.<sup>26,32</sup> The CV results suggest that the phosphine–carboxamide ligands have considerably stabilized the Ru(II) state.<sup>26,32</sup> The irreversible and/or quasi-reversible nature of the Ru<sup>3+</sup>/Ru<sup>2+</sup> redox couple suggests considerable structural changes during the process of electron transfer.

### Transfer hydrogenation

Subsequently, all three Ru(II) complexes were utilized for the TH of assorted carbonyl compounds.<sup>4–6</sup> Initially, reaction conditions were optimized by varying the solvent, base, catalyst and catalyst loading (Table 1). As can be seen from entry 1, the presence of a catalyst is critical in driving the TH reaction as its absence did not produce any product. Entries 2 and 3 show that Ru(II) precursors, such as [Ru(CO)<sub>2</sub>Cl<sub>2</sub>]<sub>*n*</sub> and [RuH(CO)Cl(PPh<sub>3</sub>)<sub>3</sub>], were largely ineffective as catalysts in promoting TH. The presence of a suitable base is essential as its absence

**Table 1** Control and optimization experiments for transfer hydrogenation reactions using acetophenone as a model substrate<sup>a</sup>



Entry	Catalyst	Base	Solvent	Yield <sup>b</sup> (%)
1	—	KOH	i-PrOH	0
2	[Ru(CO) <sub>2</sub> Cl <sub>2</sub> ] <sub><i>n</i></sub>	KOH	i-PrOH	5
3	RuH(CO)Cl(PPh <sub>3</sub> ) <sub>3</sub>	KOH	i-PrOH	4
4	2	—	i-PrOH	8
5	2	Et <sub>3</sub> N	i-PrOH	20
6	2	<sup>t</sup> BuOK	i-PrOH	35
7	2	NaOH	i-PrOH	54
8	2	KOH	i-PrOH	94
9	2	KOH	MeOH	12
10	2	KOH	EtOH	20
11	2	KOH	DMF	0
12	2	KOH	DMSO	0
13	2	KOH	THF	0
14	1	NaOH	i-PrOH	42
15	1	KOH	i-PrOH	91
16	3	NaOH	i-PrOH	48
17	3	KOH	i-PrOH	90
18 <sup>c</sup>	2	KOH	i-PrOH	85

<sup>a</sup> Conditions: Catalyst, 0.02 mmol (1 mol%); acetophenone, 2.00 mmol; KOH, 1.00 mmol; i-PrOH, 5 mL; temperature, 80 °C; time, 6 h. <sup>b</sup> Determined by gas chromatography. <sup>c</sup> 0.5 mol% catalyst loading with a reaction time of 12 h.

resulted in a miniscule TH product (entry 4). Entries 5–7 show that other bases (Et<sub>3</sub>N, <sup>t</sup>BuOK and NaOH) were only moderately successful. Satisfyingly, complex 2 in the presence of KOH as a base and isopropanol as both the solvent and hydrogen donor provided 94% of the TH product, 1-phenylethanol (entry 8). In comparison, both MeOH and EtOH had limited success (entries 9 and 10), whereas, as expected, other solvents were completely ineffective (entries 11–13).<sup>23</sup> Entries 14–17 display that complexes 1 and 3 were also effective TH catalysts with KOH as a base, although their catalytic efficiency was lower when compared to that of complex 2. When the catalyst loading of complex 2 was reduced to half, 85% product formation was observed in 12 h (entry 18), compared to that obtained in 6 h with a higher catalyst loading of 1 mol% (entry 8). In order to rule out the involvement of [Ru] nanoparticles in catalysis, the mercury drop-test was carried out.<sup>33</sup> The presence of one drop of Hg did not alter the outcome of the TH of acetophenone, producing 1-phenylethanol in 93% yield (data not shown in Table 1).<sup>33</sup> As complex 2 was a better catalyst, it was used to explore the scope of TH catalysis with a variety of carbonyl substrates (Table 2).

As can be seen from Table 2, both the electron-withdrawing and electron-donating groups on the phenyl ring of a carbonyl compound were tolerated in the aforementioned TH catalysis, producing the corresponding alcohols as the products in excellent yields (entries 1–13).<sup>4,34c,d</sup> However, it was noted that the substrates containing electron-withdrawing groups underwent faster reduction as compared to the ones having electron-donating groups.<sup>34</sup> This can be explained by correlating the

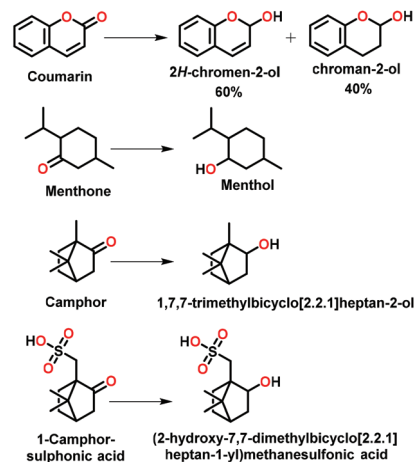
**Table 2** Substrate scope in the catalytic transfer hydrogenation reaction of assorted carbonyl compounds using complex 2 as a catalyst<sup>a</sup>

Entry	Substrate	Product	Yield <sup>b</sup> (%)
1			94
2			92
3			88
4			85
5			85
6			89
7			95
8			88
9			89
10			87
11			83
12			85
13			80
14			87
15			90

<sup>a</sup> Conditions: Substrate, 2.00 mmol; catalyst 2, 0.02 mmol; KOH, 1.00 mmol; <sup>1</sup>PrOH, 5 mL; temperature, 80 °C, time, 6 h. <sup>b</sup> Determined by gas chromatography (Fig. S36–S50, ESI<sup>†</sup>) and characterized by <sup>1</sup>H NMR spectroscopy (Fig. S51–S65, ESI<sup>†</sup>).

ease in hydride transfer from the *in situ* generated [Ru–H] intermediate to the carbonyl substrate as the electrophilicity of the carbonyl group is increased by the presence of an electron-withdrawing substituent.<sup>4–6,34</sup> Entries 14 and 15 show that cyclic ketones can be conveniently converted to their respective alcohols in high yield.

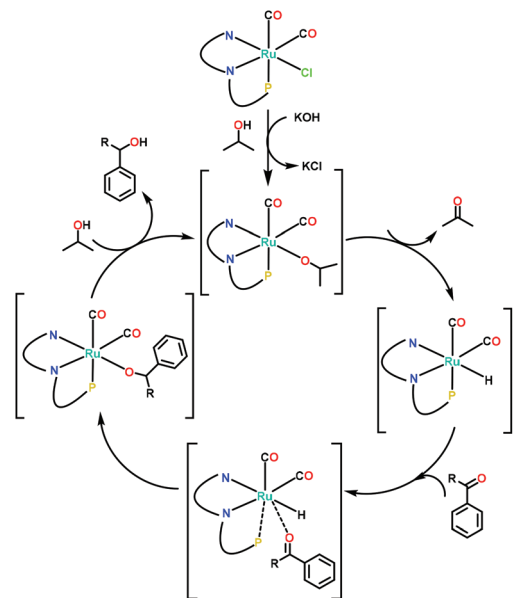
We then focussed on the TH of a few biologically relevant substrates (Scheme 2) under the optimized reaction con-

**Scheme 2** Transfer hydrogenation of some biologically relevant substrates. The yield was determined by gas chromatography (Fig. S66–S69, ESI<sup>†</sup>), whereas the products were characterized by <sup>1</sup>H NMR spectroscopy (Fig. S70–S73, ESI<sup>†</sup>).

ditions, however, with 3 mol% catalyst loading. Interestingly, the TH of coumarin resulted in complete conversion but produced both 2H-chromen-2-ol (*ca.* 60%) and chroman-2-ol (*ca.* 40%) (Fig. S70, ESI<sup>†</sup>).<sup>36</sup> Notably, menthone was quantitatively reduced (*ca.* 98%) to menthol with a 53 : 47 diastereomeric ratio as determined using the <sup>1</sup>H NMR spectrum (Fig. S71, ESI<sup>†</sup>).<sup>35</sup> Both camphor (in 77 : 23 diastereomeric ratio; Fig. S72, ESI<sup>†</sup>) and 1-camphor sulphonic acid (in 67 : 33 diastereomeric ratio; Fig. S73, ESI<sup>†</sup>) were reduced to their corresponding alcohol products in decent yields (*ca.* 60–65%).<sup>34c</sup> The success of these substrates substantiated the practical utility of the present catalysts in promoting challenging TH reactions.

### Substrate binding and mechanistic studies

Based on the literature and the present catalysis results, a tentative mechanism for TH is proposed and presented in Scheme 3.<sup>37</sup> The first step involves base-assisted displacement of the ligated chloride ion by the isopropoxide ion (<sup>−</sup>O<sup>i</sup>Pr).<sup>37</sup> The [Ru–O<sup>i</sup>Pr] species then generates the ruthenium coordinated hydride intermediate, [Ru–H], which is responsible for the hydrogenation of the carbonyl substrate.<sup>38–40</sup> In order to prove the proposed mechanism, it was essential to substantiate the generation of [Ru–O<sup>i</sup>Pr] and [Ru–H] species.<sup>41</sup> Additionally, the possible labile nature of the co-ligand, the chloride ion, in the Ru(II) complex is equally significant. Therefore, the potential replacement of the chloride ion by the isopropoxide ion was investigated by taking complexes 2 and 3 as the representative examples. The case of complex 2 is explained here. Thus, when complex 2 was titrated with potassium isopropoxide in DMF,<sup>42</sup> a clear transformation resulted as shown in Fig. 2. Prominent spectral changes were noted at 386, 454 and 536 nm for 2 as a function of the concentration of potassium isopropoxide. An isosbestic point was observed at *ca.* 440 nm, suggesting a neat transformation. Importantly, Job's plot unambiguously justified a 1 : 1 stoichiometry



**Scheme 3** Proposed catalytic cycle for the transfer hydrogenation reaction taking complex **2** as a representative example.

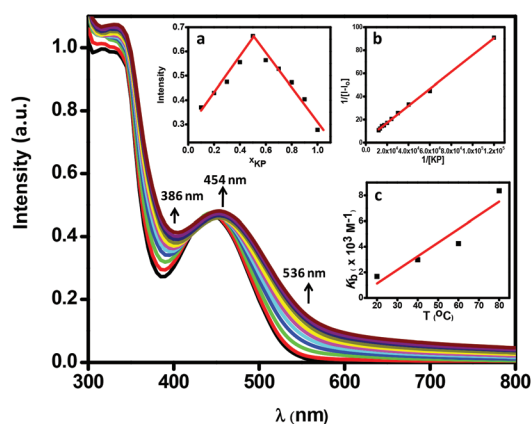


**Fig. 2** UV-Vis spectral titration of complex **2** with potassium isopropoxide. Inset a: Job's plot showing a 1 : 1 binding stoichiometry between **2** and the isopropoxide ion. Inset b: Linear regression fitting curve for a 1 : 1 binding between **2** and the isopropoxide ion at  $\lambda = 386$  nm. Inset c: Temperature dependent binding of the isopropoxide ion with **2**. All studies were performed in DMF.

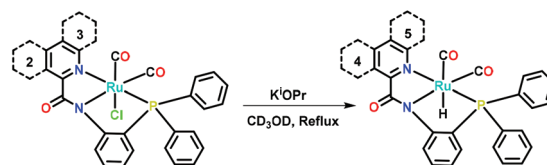
between complex **2** and the isopropoxide ion (inset a).<sup>43</sup> Such a fact was further supported by the linear regression fitting for a 1 : 1 stoichiometry between the Ru(II) complex and the  $\text{O}^i\text{Pr}$  ion (inset b).<sup>43</sup> The binding constant ( $K_b$ ) was found to be  $3.65 \times 10^3 \text{ M}^{-1}$ .<sup>44</sup> Further evidence was obtained from the temperature-dependent binding of the isopropoxide ion with complex **2** (inset c). As can be seen, the binding constant ( $K_b \times 10^3 \text{ M}^{-1}$ ) was found to increase with an increase in temperature in the following order: 1.69 (20 °C), 3.38 (40 °C), 4.46 (60 °C) and 8.35 (80 °C), showing a nearly linear relationship.<sup>45</sup> The binding of the isopropoxide ion was also investigated with

complex **3** and similar observations were noted including the binding constant of  $3.38 \times 10^3 \text{ M}^{-1}$  and a 1 : 1 stoichiometry (Fig. S74, ESI<sup>†</sup>). In addition, binding studies confirmed that the ligated  $-\text{Cl}$  ion has been replaced by the isopropoxide ion on the ruthenium center.

The next challenge was to ascertain the generation of the  $[\text{Ru}-\text{H}]$  species.<sup>38–40</sup> For such a purpose, complexes **2** and **3** were selected. Thus, when **2** and **3** were refluxed with potassium isopropoxide in  $\text{CD}_3\text{OD}$ , brown-red to red products were precipitated that were isolated. These products were respectively found to be the corresponding Ru–H complexes **4** and **5** (Scheme 4). The proton NMR spectra of **4** and **5** showed the presence of metal-bound hydride as the doublet at  $-9.48$  ( $^2J_{\text{HP}}$ : 25 Hz) and  $-10.00$  ppm ( $^2J_{\text{HP}}$ : 21 Hz), respectively (Fig. S75 and S76, ESI<sup>†</sup>).<sup>37</sup> Similarly, the  $^{13}\text{C}$  NMR spectra of **4** and **5** were somewhat similar to those of their precursors **2** and **3** although prominent shifts were noted for the ligated CO molecules (Fig. S77 and S78, ESI<sup>†</sup>). The FTIR spectra of **4** and **5** illustrated the hydride stretches at 2039 and 2020  $\text{cm}^{-1}$ , respectively, whereas most of the other stretches were quite similar to those of complexes **2** and **3** (Fig. S79 and S80, ESI<sup>†</sup>). Both complexes **4** and **5** displayed absorption maxima at 430–440 nm (Fig. S81, ESI<sup>†</sup>). Collectively, these results indicated the formation of Ru–H complexes from the *in situ* generated  $[\text{Ru}-\text{O}^i\text{Pr}]$  species.

With isolated Ru–H complexes **4** and **5** in hand, the TH of acetophenone was attempted. Importantly, both **4** and **5** were greatly successful in the TH of acetophenone producing 1-phenylethanol in quantitative yield (>99%) in 12 h. More importantly, such TH reactions were accomplished without the requirement of any base, as anticipated for the Ru–H species.<sup>37d–f</sup> These experiments unambiguously asserted that the Ru–H species is involved in the TH of the carbonyl substrate as illustrated in Scheme 3.

The isolated Ru–H complexes **4** and **5** further provided the opportunity to explore the relationship between different electronic substituents present on a substrate and the rate constant as well as the reaction yield (Fig. 3). In these experiments, the following *para*-substituents on the phenyl ring of acetophenone were utilized: H,  $\text{CH}_3$ , Cl and  $\text{NO}_2$ . Importantly, the pseudo first order rate constant ( $[K \times 10^{-3} \text{ min}^{-1}]$ )<sup>46</sup> of 7.11 ( $-\text{CH}_3$ ), 7.62 ( $-\text{H}$ ), 8.73 ( $-\text{Cl}$ ) and 9.97 ( $-\text{NO}_2$ ) varied linearly with respect to the Hammett constants ( $\sigma$ ) yielding a positive slope (blue triangles). Such a point supported the fact that the substrates with electron-withdrawing groups favored TH more than the substrates with electron-donating groups.<sup>34,37d</sup> In



**Scheme 4** Synthesis of Ru–H complexes **4** and **5** from complexes **2** and **3**.

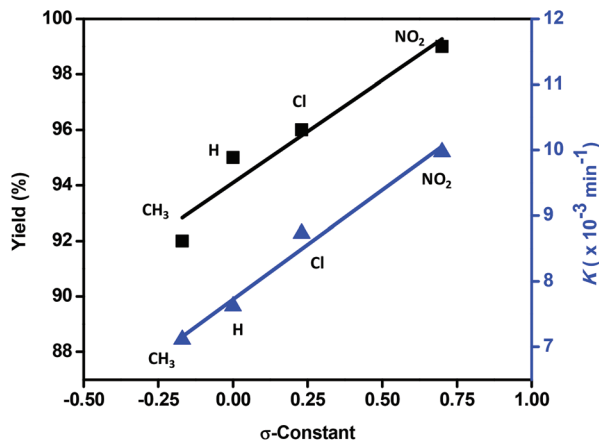


Fig. 3 Hammett plot illustrating the electronic effect of the substituents (H, CH<sub>3</sub>, Cl and NO<sub>2</sub>) at the *para* position of acetophenone on the rate constant for a pseudo first order reaction (blue triangles) and on the product yield for a 12 h TH reaction (black squares).

fact, the  $\rho$  value from the Hammett plot was not only positive but also quite large (+3.05) and supported the same.<sup>47</sup> The large positive  $\rho$  value further suggested the formation of a negatively charged transition state during the reaction which is better stabilized by the electron-withdrawing substituents. Similar large  $\rho$  values of +4.7 and +3.1 have been reported in the literature for the NaBH<sub>4</sub> mediated reduction of substituted benzaldehydes<sup>48a</sup> and acetophenones,<sup>48b</sup> respectively, implying the more anionic nature of the transition state.

Further evidence was obtained from a similar plot but involving yields (92% (–CH<sub>3</sub>), 95% (–H), 96% (–Cl) and 99% (–NO<sub>2</sub>))<sup>49</sup> of the TH reaction and the Hammett constants ( $\sigma$ ) for the four substrates (Fig. S82–S85, ESI†). Such a plot further showed a linear relationship, therefore supporting the rate constant experiment.

To support the detachment of the phosphine group as shown in Scheme 3, the time-dependent <sup>31</sup>P NMR spectra of complex 4 in the presence of a substrate, acetophenone, were studied (Fig. 4). The original <sup>31</sup>P signal for pristine 4, at 69 ppm (trace a), slowly disappeared with time, whereas two new resonances were observed at *ca.* 49 and *ca.* 28 ppm corresponding to the partially and fully detached phosphine groups of the ligand (traces b and c). This experiment therefore asserted the involvement of the inner-sphere reaction mechanism<sup>37d-f</sup> as was also inferred from the Hammett studies.

## Experimental section

### Chemicals and reagents

All chemicals and reagents were obtained from commercial sources and were used without further purification. 2-Aminodiphenylphosphine was synthesized using the reported method.<sup>50</sup> [Ru(CO)<sub>2</sub>(Cl)<sub>2</sub>]<sub>n</sub> was synthesized as per the literature method.<sup>51</sup>

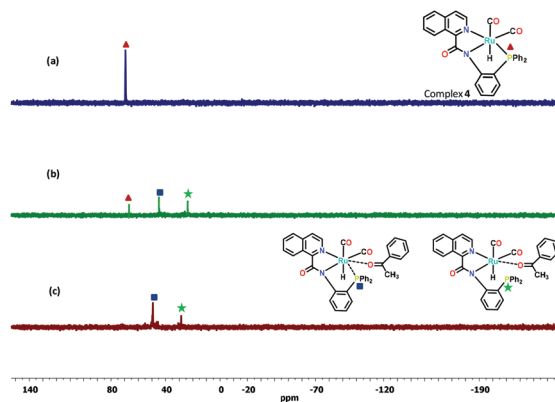


Fig. 4 Selected part of the <sup>31</sup>P NMR spectrum of complex 4 in DMSO-d<sub>6</sub> showing <sup>31</sup>P peaks (a) at 69 ppm for pristine complex 4 and in the presence of an equimolar amount of acetophenone after heating at 80 °C for (b) 1 h and (c) 6 h.

### Synthesis of ligands

**N-(2-(Diphenylphosphino)phenyl)pyridine-1-carboxamide (HL<sup>1</sup>).** 2-Aminodiphenylphosphine (1.00 g, 3.60 mmol) and 2-picolinic acid (0.443 g, 3.61 mmol) were taken in 5 ml of pyridine and stirred at 100 °C followed by the addition of triphenylphosphite (1.34 g, 4.30 mmol). After stirring the reaction mixture for 12 h at 100 °C, the solvent was removed under reduced pressure. The crude oily product thus obtained was washed several times with cold water. The addition of diethyl ether afforded an off-white product. Yield: 1.28 g (92%). Anal. calcd for C<sub>24</sub>H<sub>19</sub>N<sub>2</sub>OP (382.39): C 75.38, H 5.01, N 7.33; found C 75.10, H 5.12, N 7.13. FTIR spectrum (Zn–Se ATR, cm<sup>-1</sup>): 3386 (O–H), 3271 (N–H), 3054 (C–H), 1688 (C=O<sub>asym</sub>), 1527 (C=O<sub>sym</sub>), 1431 (C=C), 694 (C–H<sub>bending</sub>). <sup>1</sup>H NMR spectrum (400 MHz, CDCl<sub>3</sub>, 25 °C):  $\delta$  (ppm) 10.85 (s), 8.54 (d,  $J = 4.8$  Hz), 8.46 (dd,  $J = 8.2, 4.6$  Hz), 8.18 (d,  $J = 6.9$  Hz), 7.81 (t,  $J = 7.7$  Hz), 7.37 (ddd,  $J = 12.8, 8.1, 4.1$  Hz), 7.07 (t,  $J = 7.4$  Hz), 6.98–6.90 (m). <sup>13</sup>C NMR spectrum (100 MHz, CDCl<sub>3</sub>, 25 °C):  $\delta$  (ppm) 162.20, 150.04, 148.14, 141.03, 140.92, 137.46, 134.91, 134.16, 133.97, 133.87, 132.28, 130.22, 129.21, 128.77, 128.70, 127.47, 126.34, 124.74, 122.31 and 121.52. <sup>31</sup>P NMR spectrum (160 MHz, CDCl<sub>3</sub>, 25 °C):  $\delta$  (ppm) –19.23. MS spectrum (ESI<sup>+</sup>):  $m/z$  calcd for [C<sub>24</sub>H<sub>20</sub>N<sub>2</sub>OP]<sup>+</sup> 383.40, found 383.13.

**N-(2-(Diphenylphosphino)phenyl)isoquinoline-3-carboxamide (HL<sup>2</sup>).** A similar method (as for HL<sup>1</sup>) was adopted with the following reagents: 2-aminodiphenylphosphine (1.00 g, 3.60 mmol), isoquinoline-1-carboxylic acid (0.62 g, 3.60 mmol) and triphenylphosphite (1.10 g, 3.60 mmol). The isolated crude product was dissolved in acetone and stored at 0 °C to afford a pale pink crystalline product. Yield: 1.35 g (86%). Anal. calcd for C<sub>28</sub>H<sub>21</sub>N<sub>2</sub>OP (432.45): C 77.77, H 4.89, N 6.48; found C 77.83, H 5.00, N 6.61. FTIR spectrum (Zn–Se ATR, cm<sup>-1</sup>): 3226 (N–H), 3046 (C–H), 1678 (C=O<sub>asym</sub>), 1578 (C=O<sub>sym</sub>), 1427 (C=C), 695 (C–H<sub>bending</sub>). <sup>1</sup>H NMR spectrum (400 MHz, CDCl<sub>3</sub>, 25 °C):  $\delta$  (ppm) 10.99 (s), 9.58 (d,  $J = 8.4$  Hz), 8.42 (d,  $J = 5.5$  Hz), 7.85 (dd,  $J = 21.1, 6.4$  Hz), 7.72–7.61 (m), 7.46 (t,  $J = 7.1$  Hz), 7.40–7.26 (m), 7.09 (t,  $J = 7.4$  Hz), 7.00–6.94

(m).  $^{13}\text{C}$  NMR spectrum (100 MHz,  $\text{CDCl}_3$ , 25 °C):  $\delta$  (ppm) 162.29, 149.66, 146.32, 141.00, 140.81, 137.31, 135.02, 134.94, 134.19, 133.99, 133.84, 130.25, 130.19, 130.06, 129.42, 129.25, 128.86, 128.78, 128.17, 127.72, 124.78, 121.56 and 118.72.  $^{31}\text{P}$  NMR spectrum (160 MHz,  $\text{CDCl}_3$ , 25 °C)  $\delta$  (ppm) -17.96. MS spectrum ( $\text{ESI}^+$ ):  $m/z$  calcd for  $[\text{C}_{28}\text{H}_{22}\text{N}_2\text{OP}]^+$  433.14, found 433.02.

***N*-(2-(Diphenylphosphino)phenyl)quinoline-3-carboxamide (HL<sup>3</sup>)**. A similar method (as for HL<sup>1</sup>) was adopted with the following reagents: 2-aminodiphenylphosphine (1.00 g, 3.60 mmol), quinoline-2-carboxylic acid (0.62 g, 3.60 mmol) and triphenylphosphite (1.10 g, 3.60 mmol). The isolated crude product was dissolved in acetone and stored at 0 °C to afford an orange crystalline product. Yield: 1.35 g (87%). Anal. calcd for  $\text{C}_{28}\text{H}_{21}\text{N}_2\text{OP}$  (432.45): C 77.77, H 4.89, N 6.48; found C 77.80, H 5.09, N 6.69. FTIR spectrum (Zn–Se ATR,  $\text{cm}^{-1}$ ): 3355 (O–H), 3235 (N–H), 3047 (C–H), 1679 (C=O<sub>asym</sub>), 1569 (C=O<sub>sym</sub>), 1433 (C=C), 694 (C–H<sub>bending</sub>).  $^1\text{H}$  NMR spectrum (400 MHz,  $\text{CDCl}_3$ , 25 °C):  $\delta$  (ppm) 11.06 (s), 8.50 (dd,  $J = 8.2$ , 4.6 Hz), 8.05 (d,  $J = 8.4$  Hz), 7.85 (d,  $J = 7.4$  Hz), 7.76 (t,  $J = 7.7$  Hz), 7.61 (t,  $J = 7.5$  Hz), 7.42–7.24 (m), 7.09 (t,  $J = 7.5$  Hz), 7.00–6.97 (m).  $^{13}\text{C}$  NMR spectrum (100 MHz,  $\text{CDCl}_3$ , 25 °C):  $\delta$  (ppm) 163.75, 140.11, 137.61, 134.96, 134.87, 134.33, 134.21, 134.02, 133.74, 130.56, 130.10, 129.22, 128.84, 128.79, 128.71, 128.57, 127.77, 127.77, 127.27, 126.97, 124.78, 124.73, and 121.91.  $^{31}\text{P}$  NMR spectrum (160 MHz,  $\text{CDCl}_3$ , 25 °C)  $\delta$  (ppm) -18.58. MS spectrum ( $\text{ESI}^+$ ):  $m/z$  calcd for  $[\text{C}_{28}\text{H}_{22}\text{N}_2\text{OP}]^+$  433.14, found 433.02.

### Synthesis of Ru(II) complexes

**$[\text{Ru}(\text{L}^1)(\text{CO})(\text{Cl})(\text{CH}_3\text{OH})]$  (1)**. Ligand HL<sup>1</sup> (0.084 g, 0.22 mmol) was dissolved in methanol (15 mL) followed by the addition of  $[\text{Ru}(\text{CO})_2(\text{Cl})_2]_n$  (0.050 g, 0.22 mmol) and the reaction mixture was refluxed for 12 h. After that the solvent was removed under reduced pressure. The yellow crude product was isolated after washing thrice with diethyl ether. The crude product was recrystallized from methanol after layering with diethyl ether that produced the crystalline product within 2–3 days. Yield: 0.105 g (83%). Anal. calcd for  $\text{C}_{26}\text{H}_{22}\text{N}_2\text{O}_3\text{P}(\text{Cl})\text{Ru}$  (577.97): C 54.03, H 3.84, N 4.85; found: 54.20, H 3.65, N 4.71; FTIR spectrum (Zn–Se ATR,  $\text{cm}^{-1}$ ): 3390 (O–H<sub>MeOH</sub>), 3058 ( $\nu_{\text{C-H}}$ ), 1939 ( $\nu_{\text{CO}}$ ), 1620 ( $\nu_{\text{C=O}_{\text{asym}}}$ ), 1460 ( $\nu_{\text{C=O}_{\text{sym}}}$ ), 1428 ( $\nu_{\text{C-H}}$ , bending). UV/Vis spectrum (DMF,  $\lambda_{\text{max}}$  ( $\epsilon$ ,  $\text{mol}^{-1}\text{cm}^{-1}$ ): 365.  $^1\text{H}$  NMR spectrum (400 MHz,  $\text{CDCl}_3$ , 25 °C):  $\delta$  (ppm) 9.57 (dd,  $J = 8.6$ , 5.4 Hz), 8.65 (s), 8.34 (d,  $J = 7.9$  Hz), 8.03 (t,  $J = 7.8$  Hz), 7.92 (dd,  $J = 12.2$ , 6.9 Hz), 7.55 (ddd,  $J = 21.5$ , 11.5, 4.9 Hz), 7.47–7.42 (m), 7.32 (dd,  $J = 10.5$ , 8.5 Hz), 7.16 (t,  $J = 7.4$  Hz), 3.46 (s).  $^{13}\text{C}$  NMR spectrum (100 MHz,  $\text{CDCl}_3$ , 25 °C):  $\delta$  207.11, 167.48, 152.39, 137.56, 136.02, 130.67, 130.57, 129.10, 128.91, 127.95, 127.77, 127.62, 126.06, 121.73, 120.91, 119.05, 87.21 and 49.44.  $^{31}\text{P}$  NMR spectrum (160 MHz,  $\text{CDCl}_3$ , 25 °C):  $\delta$  (ppm) 46.17. MS spectrum ( $\text{ESI}^+$ ,  $\text{CH}_3\text{OH}$ ):  $m/z$  calcd for  $[\text{C}_{25}\text{H}_{19}\text{N}_2\text{O}_3\text{P}(\text{Cl})\text{Ru}]^+$  546.99, found 546.9924.

**$[\text{Ru}(\text{L}^2)(\text{CO})_2(\text{Cl})]$  (2)**. A similar method as mentioned for complex 1 was adopted using the following reagents: ligand HL<sup>2</sup> (0.047 g, 0.110 mmol) and  $[\text{Ru}(\text{CO})_2(\text{Cl})_2]_n$  (0.025 g,

0.1101 mmol). Yield: 0.052 g (75%) Anal. calcd for  $\text{C}_{30}\text{H}_{20}\text{N}_2\text{O}_3\text{P}(\text{Cl})\text{Ru}$  (623.99): C 57.75, H 3.23, N 4.49; found: C 57.56, H 3.12, N 4.21. FTIR spectrum (Zn–Se ATR,  $\text{cm}^{-1}$ ): 3048 ( $\nu_{\text{C-H}}$ ), 2049 ( $\nu_{\text{CO}}$ ), 1984 ( $\nu_{\text{CO}}$ ), 1627 ( $\nu_{\text{C=O}}$ ). UV/Vis spectrum (DMF,  $\lambda_{\text{max}}$  ( $\epsilon$ ,  $\text{mol}^{-1}\text{cm}^{-1}$ ): 430.  $^1\text{H}$  NMR spectrum (400 MHz,  $\text{CDCl}_3$ , 25 °C):  $\delta$  (ppm) 10.36–10.26 (d), 9.66–9.56 (dd), 8.55 (dd,  $J = 6.1$ , 2.8 Hz), 7.97–7.77 (m), 7.64–7.54 (m), 7.51–7.42 (m), 7.35 (ddd,  $J = 11.3$ , 7.7, 1.5 Hz), 7.20–7.15 (m).  $^{13}\text{C}$  NMR spectrum (100 MHz,  $\text{CDCl}_3$ , 25 °C):  $\delta$  195.52, 190.75, 172.26, 156.33, 155.47, 144.54, 137.82, 133.16, 132.44, 131.86, 131.42, 130.99, 130.11, 129.70, 129.08, 128.66, 128.19, 127.19, 124.69, 123.41, 122.95 and 122.22.  $^{31}\text{P}$  NMR spectrum (160 MHz,  $\text{CDCl}_3$ , 25 °C):  $\delta$  (ppm) 47.89. MS spectrum ( $\text{ESI}^+$ ,  $\text{CH}_3\text{OH}$ ):  $m/z$  calcd for  $[\text{C}_{30}\text{H}_{20}\text{N}_2\text{O}_3\text{P}(\text{Cl})\text{Ru} + \text{H}^+]$  625.

**$[\text{Ru}(\text{L}^3)(\text{CO})_2(\text{Cl})]$  (3)**. A similar method as discussed for complex 1 was followed using the following reagents: ligand HL<sup>3</sup> (0.047 g, 0.1101 mmol) and  $[\text{Ru}(\text{CO})_2(\text{Cl})_2]_n$  (0.025 g, 0.1101 mmol). Yield: 0.052 g (75%) Anal. calcd for  $\text{C}_{30}\text{H}_{20}\text{N}_2\text{O}_3\text{P}(\text{Cl})\text{Ru}$  (623.99): C 57.75, H 3.23, N 4.49; found: C 57.66, H 3.41, N 4.23. FTIR spectrum (Zn–Se ATR,  $\text{cm}^{-1}$ ): 3046 ( $\nu_{\text{CH}}$ ), 2043 ( $\nu_{\text{CO}}$ ), 1974 ( $\nu_{\text{CO}}$ ), 1650 ( $\nu_{\text{C=O}}$ ). UV/Vis spectrum (DMF,  $\lambda_{\text{max}}$  ( $\epsilon$ ,  $\text{mol}^{-1}\text{cm}^{-1}$ ): 401.  $^1\text{H}$  NMR spectrum (400 MHz,  $\text{CDCl}_3$ , 25 °C)  $\delta$  (ppm) 9.56 (dd,  $J = 8.5$ , 5.5 Hz), 8.53 (ddd,  $J = 18.3$ , 15.0, 8.6 Hz), 8.05–7.90 (m), 7.72 (ddd,  $J = 8.0$ , 7.1, 0.9 Hz), 7.61 (dt,  $J = 14.1$ , 4.3 Hz), 7.56–7.42 (m), 7.39–7.29 (m), 7.22–7.14 (m).  $^{13}\text{C}$  NMR spectrum (100 MHz,  $\text{CDCl}_3$ , 25 °C):  $\delta$  197.11, 189.95, 169.02, 160.41, 156.04, 145.97, 140.44, 134.81, 134.62, 133.58, 133.42, 132.16, 131.67, 131.26, 129.20, 129.15, 128.76, 128.66, 128.16, 125.00, 123.64, 122.00.  $^{31}\text{P}$  NMR spectrum (160 MHz,  $\text{CDCl}_3$ , 25 °C):  $\delta$  (ppm) 49.63. MS spectrum ( $\text{ESI}^+$ ,  $\text{CH}_3\text{OH}$ ):  $m/z$  calcd for  $[\text{C}_{30}\text{H}_{20}\text{N}_2\text{O}_3\text{P}(\text{Cl})\text{Ru} + \text{H}^+]$  625.

**$[\text{Ru}(\text{L}^2)(\text{CO})_2(\text{H})]$  (4)**. Complex 2 (0.050 g, 0.08 mmol) was treated with  $\text{KO}^i\text{Pr}$  (0.063 g, 0.91 mmol) in  $\text{CD}_3\text{OD}$  (1 mL) and refluxed at 70 °C for about an hour. A reddish-brown precipitate was obtained which was isolated by filtration and dried under vacuum. Yield 0.020 g (65%). Anal. calcd for  $\text{C}_{30}\text{H}_{21}\text{N}_2\text{O}_3\text{P}(\text{H})\text{Ru}$  (589.55): C 57.75, H 3.23, N 4.49; found: C 57.66, H 3.41, N 4.23. FTIR spectrum (Zn–Se ATR,  $\text{cm}^{-1}$ ): 2039 ( $\nu_{\text{Ru-H}}$ ), 1927 ( $\nu_{\text{CO}}$ ), 1910 ( $\nu_{\text{CO}}$ ), 1610 ( $\nu_{\text{C=O}}$ ). UV/Vis spectrum (DMF,  $\lambda_{\text{max}}$  ( $\epsilon$ ,  $\text{mol}^{-1}\text{cm}^{-1}$ ): 442.  $^1\text{H}$  NMR spectrum (400 MHz, DMSO, 25 °C):  $\delta$  (ppm) 10.17 (d,  $J = 8.7$  Hz, 1H), 9.42 (dd,  $J = 8.4$ , 4.8 Hz, 1H), 8.77 (d,  $J = 6.0$  Hz, 1H), 8.13 (t,  $J = 7.1$  Hz, 2H), 8.00–7.88 (m, 3H), 7.85 (d,  $J = 8.4$  Hz, 1H), 7.61–7.39 (m, 10H), 7.16 (t,  $J = 7.3$  Hz, 1H), -9.48 (d,  $J = 25.0$  Hz, 1H).  $^{13}\text{C}$  NMR spectrum (100 MHz, DMSO, 25 °C):  $\delta$  211.32, 206.17, 169.39, 159.46, 156.63, 145.88, 139.85, 137.82, 133.64, 133.55, 133.33, 131.54, 130.52, 130.12, 129.70, 129.37, 128.99, 128.82, 128.68, 125.79, 123.31, 122.49.

**$[\text{Ru}(\text{L}^3)(\text{CO})_2(\text{H})]$  (5)**. A similar method on an identical scale, as discussed for complex 4, was followed using complex 3. A red coloured product was isolated. Yield 0.026 g (74%). Anal. calcd for  $\text{C}_{30}\text{H}_{21}\text{N}_2\text{O}_3\text{P}(\text{H})\text{Ru}$  (589.55): C 57.75, H 3.23, N 4.49; found: C 58.06, H 3.15, N 4.55. FTIR spectrum (Zn–Se ATR,  $\text{cm}^{-1}$ ) 2020 ( $\nu_{\text{Ru-H}}$ ), 1910 ( $\nu_{\text{CO}}$ ), 1906 ( $\nu_{\text{CO}}$ ), 1615 ( $\nu_{\text{C=O}}$ ). UV/Vis spectrum (DMF,  $\lambda_{\text{max}}$  ( $\epsilon$ ,  $\text{mol}^{-1}\text{cm}^{-1}$ ): 430.  $^1\text{H}$  NMR spectrum (400 MHz, DMSO, 25 °C):  $\delta$  (ppm) 9.41 (dd,  $J = 8.3$ , 4.7 Hz,

1H), 8.78 (t,  $J = 9.3$  Hz, 2H), 8.36 (d,  $J = 8.4$  Hz, 1H), 8.21 (d,  $J = 8.1$  Hz, 1H), 8.06 (t,  $J = 7.7$  Hz, 1H), 7.98–7.92 (m, 2H), 7.84 (t,  $J = 7.4$  Hz, 1H), 7.57–7.46 (m, 10H), 7.17 (t,  $J = 7.3$  Hz, 1H), –10.00 (d,  $J = 21$  Hz, 1H).  $^{13}\text{C}$  NMR spectrum (100 MHz, DMSO, 25 °C):  $\delta$  210.76, 204.52, 168.72, 160.04, 155.63, 147.02, 140.11, 135.92, 135.57, 134.19, 133.16, 132.25, 131.90, 130.25, 129.48, 129.09, 126.04, 123.85, 123.26, 122.61.

### General procedure for the transfer hydrogenation of carbonyl substrates

A reaction mixture of 1 mol% catalyst, carbonyl substrate (2 mmol) and KOH (1 mmol) in isopropyl alcohol (5 mL) was stirred at 80 °C for 6 h. After cooling, the mixture was diluted with water and then extracted with ethyl acetate. The organic layer was separated, washed with aqueous brine and dried over anhyd.  $\text{Na}_2\text{SO}_4$ . The removal of the solvent under reduced pressure afforded an organic product that was purified by column chromatography on neutral alumina using 5% ethyl acetate/hexanes solution. The organic products were identified by gas chromatography (GC). A calibration plot was studied for a mixture of 4-nitro acetophenone (substrate) and 1-(4-nitrophenyl)ethan-1-ol (product) and is presented in Fig. S86 (ESI†).

### NMR spectral characterization data for TH organic products

**1-Phenylethan-1-ol.**  $^1\text{H}$  NMR spectrum (400 MHz,  $\text{CDCl}_3$ , 25 °C):  $\delta$  (ppm) 7.34 (d, 3H), 7.27 (m, 1H), 4.89 (q,  $J = 6.5$  Hz, 1H), 1.49 (d,  $J = 6.5$  Hz, 3H).

**Diphenylmethanol.**  $^1\text{H}$  NMR spectrum (400 MHz,  $\text{CDCl}_3$ , 25 °C):  $\delta$  (ppm) 7.41–7.29 (m, 8H), 7.28–7.22 (m, 2H), 5.82 (s, 1H).

**1-(*p*-Tolyl)ethan-1-ol.**  $^1\text{H}$  NMR spectrum (400 MHz,  $\text{CDCl}_3$ , 25 °C):  $\delta$  (ppm) 7.26 (d,  $J = 8.1$  Hz, 2H), 7.15 (d,  $J = 7.9$  Hz, 2H), 4.85 (q,  $J = 6.4$  Hz, 1H), 2.34 (s, 3H), 1.47 (d,  $J = 6.5$  Hz, 3H).

**1-(4-Chlorophenyl)ethan-1-ol.**  $^1\text{H}$  NMR spectrum (400 MHz,  $\text{CDCl}_3$ , 25 °C):  $\delta$  (ppm) 7.41–7.26 (m, 4H), 4.87 (q,  $J = 6.5$  Hz, 1H), 1.46 (d,  $J = 6.4$  Hz, 3H).

**1-(4-Bromophenyl)ethan-1-ol.**  $^1\text{H}$  NMR spectrum (400 MHz,  $\text{CDCl}_3$ , 25 °C):  $\delta$  (ppm) 7.31 (d,  $J = 8.3$  Hz, 2H), 7.22 (d,  $J = 7.7$  Hz, 2H), 4.91 (q,  $J = 6.5$  Hz, 1H), 1.50 (d,  $J = 6.6$  Hz, 3H).

**1-(3-Bromophenyl)ethan-1-ol.**  $^1\text{H}$  NMR spectrum (400 MHz,  $\text{CDCl}_3$ , 25 °C):  $\delta$  (ppm) 7.34–7.28 (m, 3H), 7.25 (t, 1H), 4.9 (q, 1H), 1.49 (d,  $J = 6.5$  Hz, 3H).

**1-(4-Nitrophenyl)ethan-1-ol.**  $^1\text{H}$  NMR spectrum (400 MHz,  $\text{CDCl}_3$ , 25 °C):  $\delta$  (ppm) 8.20 (d,  $J = 8.7$  Hz, 2H), 7.55 (d,  $J = 8.7$  Hz, 2H), 5.03 (q,  $J = 6.5$  Hz, 1H), 1.52 (d,  $J = 6.5$  Hz, 3H).

**1-(2-Aminophenyl)ethan-1-ol.**  $^1\text{H}$  NMR spectrum (400 MHz,  $\text{CDCl}_3$ , 25 °C):  $\delta$  (ppm) 7.06 (d,  $J = 7.5$  Hz, 2H), 6.71 (t,  $J = 7.4$  Hz, 1H), 6.64 (d,  $J = 7.9$  Hz, 1H), 4.88 (q,  $J = 6.6$  Hz, 1H), 1.55 (d,  $J = 6.6$  Hz, 3H).

**1-(2,4-Dichlorophenyl)ethan-1-ol.**  $^1\text{H}$  NMR spectrum (400 MHz,  $\text{CDCl}_3$ , 25 °C):  $\delta$  (ppm) 7.39 (m, 3H), 4.8 (q,  $J = 6.6$  Hz, 1H), 1.48 (d,  $J = 6.5$  Hz, 3H).

**(4-Chlorophenyl)(phenyl)methanol.**  $^1\text{H}$  NMR spectrum (400 MHz,  $\text{CDCl}_3$ , 25 °C):  $\delta$  (ppm) 7.33 (d,  $J = 4.3$  Hz, 4H), 7.29 (d,  $J = 1.7$  Hz, 4H), 7.26 (dd,  $J = 5.2, 2.6$  Hz, 1H), 5.81 (s, 1H).

**(2-Amino-5-chlorophenyl)(phenyl)methanol.**  $^1\text{H}$  NMR spectrum (400 MHz,  $\text{CDCl}_3$ , 25 °C):  $\delta$  (ppm) 7.34 (m,  $J = 1.7, 5.2$  Hz, 8H), 5.80 (s, 1H), 3.48 (s, 1H).

**(2-Aminophenyl)(phenyl)methanol.**  $^1\text{H}$  NMR spectrum (400 MHz,  $\text{CDCl}_3$ , 25 °C):  $\delta$  (ppm) 8.18 (d,  $J = 8.3$  Hz, 1H), 7.87 (d,  $J = 8.4$  Hz, 1H), 7.72 (d,  $J = 15.4$  Hz, 1H), 7.56–7.42 (m, 6H), 7.27 (s, 1H).

**Bis(4-methoxyphenyl)methanol.**  $^1\text{H}$  NMR spectrum (400 MHz,  $\text{CDCl}_3$ , 25 °C):  $\delta$  (ppm) 7.27 (d,  $J = 9.0$  Hz), 6.85 (d,  $J = 9.0$  Hz), 5.76 (s), 3.78 (s).

**Cyclohexanol.**  $^1\text{H}$  NMR spectrum (400 MHz,  $\text{CDCl}_3$ , 25 °C):  $\delta$  (ppm) 3.61 (dd,  $J = 8.7, 4.5$  Hz, 1H), 1.89 (d,  $J = 5.5$  Hz, 2H), 1.79–1.72 (m, 2H), 1.55 (d,  $J = 11.7$  Hz, 1H), 1.27 (d,  $J = 8.5$  Hz, 5H).

**Cycloheptanol.**  $^1\text{H}$  NMR spectrum (400 MHz,  $\text{CDCl}_3$ , 25 °C):  $\delta$  (ppm) 3.94–3.72 (m, 1H), 1.81 (d,  $J = 11.0$  Hz, 2H), 1.67 (dd,  $J = 14.7, 6.3$  Hz, 3H), 1.55–1.44 (m, 7H).

**2H-Chromen-2-ol and chroman-2-ol.**  $^1\text{H}$  NMR (400 MHz,  $\text{CDCl}_3$ ):  $\delta$  (ppm) 12.41 (s), 9.35 (s), 8.72 (d,  $J = 8.4$  Hz), 8.63 (s), 7.82 (s), 7.78 (d,  $J = 5.5$  Hz), 7.67 (d,  $J = 5.5$  Hz), 7.47 (d,  $J = 7.5$  Hz), 7.41 (d,  $J = 7.6$  Hz), 7.08 (s), 6.98 (s), 5.82 (d,  $J = 10.2$  Hz), 5.78 (d,  $J = 10.2$  Hz), 5.06 (s), 5.00 (s), 4.96 (s), 4.91 (d,  $J = 8.2$  Hz), 4.30 (d,  $J = 6.7$  Hz), 4.06 (d,  $J = 6.8$  Hz), 2.88–2.81 (m), 2.58 (dd,  $J = 14.1, 5.5$  Hz).

**Menthol.**  $^1\text{H}$  NMR (400 MHz,  $\text{CDCl}_3$ ): NMR (400 MHz,  $\delta$  (ppm) 3.44–3.40 (m), 3.40–3.35 (m), 2.20–2.15 (m), 2.14 (dd,  $J = 7.1, 3.0$  Hz), 1.99–1.95 (m), 1.96–1.91 (m), 1.67 (dd,  $J = 5.6, 3.0$  Hz), 1.62 (dd,  $J = 6.7, 3.6$  Hz), 1.59 (dd,  $J = 8.1, 4.8$  Hz), 1.58 (dd,  $J = 6.6, 3.2$  Hz), 1.47–1.40 (m), 1.41–1.34 (m), 1.14–1.10 (m), 1.10–1.06 (m), 0.99 (dd,  $J = 11.7, 3.8$  Hz), 0.95 (d,  $J = 1.2$  Hz), 0.92 (s), 0.89 (s), 0.80 (s), 0.78 (s).

**1,7,7-Trimethylbicyclo[2.2.1]heptan-2-ol.**  $^1\text{H}$  NMR (400 MHz,  $\text{CDCl}_3$ )  $\delta$  (ppm) 3.99–3.90 (m), 3.57 (dd,  $J = 7.3, 4.1$  Hz), 2.32 (t,  $J = 3.4$  Hz), 2.04 (t,  $J = 4.5$  Hz), 1.94–1.91 (m), 1.89 (dd,  $J = 8.3, 4.0$  Hz), 1.81 (s), 1.77 (s), 1.68 (d,  $J = 4.1$  Hz), 1.66 (s), 1.63 (d,  $J = 3.9$  Hz), 1.60 (d,  $J = 3.5$  Hz), 1.43 (d,  $J = 3.1$  Hz), 1.41–1.39 (m), 1.39–1.36 (m), 1.32 (dd,  $J = 5.1, 3.0$  Hz), 1.28 (d,  $J = 3.6$  Hz), 1.26 (d,  $J = 3.8$  Hz), 1.19 (s), 0.96 (s), 0.93 (d,  $J = 1.9$  Hz), 0.90 (s), 0.86 (s), 0.85 (s), 0.81 (s), 0.80 (s), 0.78 (s), 0.76 (s).

**(2-Hydroxy-7,7-dimethylbicyclo[2.2.1]heptan-1-yl)methanesulfonic acid.**  $^1\text{H}$  NMR (400 MHz,  $\text{CDCl}_3$ )  $\delta$  (ppm) 3.36 (d,  $J = 20.1$  Hz, 2H), 3.27 (d,  $J = 17.8$  Hz, 1H), 2.90 (d,  $J = 8.4$  Hz, 2H), 2.78 (d,  $J = 11.6$  Hz, 1H), 2.46 (s, 2H), 2.30 (d,  $J = 16.4$  Hz, 1H), 2.02 (s, 2H), 1.88 (s, 1H), 1.63 (s, 4H), 1.41 (s, 2H), 1.27 (s, 1H), 1.11 (d,  $J = 5.3$  Hz, 2H), 1.06 (dd,  $J = 46.5, 8.8$  Hz, 12H), 0.78 (d,  $J = 14.4$  Hz, 6H).

### Physical methods

The conductivity measurements were done in DMF using the digital conductivity bridge from Popular Traders, India (model number: PT-825). Elemental analysis data were obtained using an Elementar Analysen System GmbH Vario EL-III instrument. NMR measurements were done using a 400 MHz JEOL instrument. FTIR spectra (Zn–Se ATR) were recorded using a PerkinElmer Spectrum-Two FTIR spectrometer. The absorption spectra were recorded using a PerkinElmer Lambda 950

spectrophotometer. Cyclic voltammetric experiments were performed using a CHI electrochemical analyzer (Model 1120 A). The cell contained a glassy-carbon or Pt-disc working electrode, a Pt wire auxiliary electrode and a Ag/Ag<sup>+</sup> reference electrode.<sup>52,53</sup> The solution concentrations were *ca.* 1 mM in complex and *ca.* 0.1 M in tetrabutyl ammonium perchlorate (TBAP).

### Crystallography

X-ray crystallographic data for all three complexes were collected at 298 K with an Oxford CCD diffractometer having an X-calibur sapphire measurement device equipped with a graphite monochromatic MoK $\alpha$  radiation source ( $\lambda = 0.71073$  Å).<sup>54</sup> The structures were initially solved by direct methods using SIR-92<sup>55</sup> and then further refined by full-matrix least-squares refinement techniques on  $F^2$  using SHELXL-97.<sup>56</sup> All the calculations were done in the WinGX crystallographic module.<sup>57</sup> The non-hydrogen atoms were refined anisotropically, whereas all hydrogen atoms were placed at the calculated positions in the last cycle of the refinement process. In complex **1**, attempts to assign the peaks of electron density as ghost peaks near the metal center were unsuccessful. The crystallographic data collection details and structural solution parameters are presented in Table S1 (ESI<sup>†</sup>).

### Kinetics

Kinetics experiments were performed using the UV-Vis spectral titration of complex **4** with different *para*-substituted acetophenones.<sup>58</sup> In the experiment, 40  $\mu$ M solution of complex **4** was taken followed by the gradual addition of aliquots (4  $\mu$ M) of acetophenone at an interval of one minute. The change in the absorption spectra was measured at  $\lambda_{\text{max}} = 440$  nm. Subsequently, a graph was plotted between the logarithm of the change in the absorbance with time and the slope provided the value of the rate constant. The respective rate constants were plotted against the  $\sigma$  values for the electronic substituents:  $-0.17$  (CH<sub>3</sub>),  $0$  (H),  $0.23$  (Cl),  $0.77$  (NO<sub>2</sub>).<sup>59,60</sup> All studies were performed in DMF solvent at 20 °C.

## Conclusions

This work presented ruthenium complexes of phosphine-carboxamide based tridentate ligands also containing other monodentate co-ligands. These Ru(II) complexes have been thoroughly characterized spectroscopically and crystallographically. These Ru(II) complexes were successfully utilized as homogeneous catalysts for the transfer hydrogenation of assorted carbonyl substrates including some biologically relevant substrates. The present catalysts tolerated both electron-withdrawing and electron-donating groups on a substrate producing the corresponding alcohols as exclusive products. The mechanistic investigations including binding studies illustrated the coordination of the isopropoxide ion by replacing a ligated chloride ion on the Ru(II) center before the generation

of the Ru-H intermediate that was isolated and characterized and was found to participate in the catalysis. The straightforward ruthenium complexes exhibiting significant TH catalytic performance suggest their potential in other challenging organic transformations that are presently being explored in the laboratory.

## Conflicts of interest

There are no conflicts to declare.

## Acknowledgements

RG gratefully acknowledges the Council of Scientific & Industrial Research, New Delhi (01(2841)/16/EMR-II) and the IoE Project from the University of Delhi for financial support. The authors thank CIF-USIC of the University of Delhi for the instrumental facilities. SY and PV respectively thank CSIR, New Delhi for the JRF and SERB, New Delhi for N-PDF fellowships. Reviewers' comments were very helpful during the revision stage.

## References

- 1 Y. Wei, X. Wu, C. Wang and J. Xiao, *Catal. Today*, 2015, **247**, 104–116.
- 2 J. G. de Vries and C. J. Elsevier, *Handbook of Homogeneous Hydrogenation*, Wiley-VCH, Weinheim, 2007.
- 3 Y.-Y. Li, S.-L. Yu, W.-Y. Shen and J.-X. Gao, *Acc. Chem. Res.*, 2015, **48**, 2587–2598.
- 4 G. Brieger and T. J. Nestrick, *Chem. Rev.*, 1974, **74**, 567–580.
- 5 D. Wang and D. Astruc, *Chem. Rev.*, 2015, **115**, 6621–6686.
- 6 G. Zassinovich, G. Mestroni and S. Gladiali, *Chem. Rev.*, 1992, **92**, 1051–1069.
- 7 R. Noyori and S. Hashiguchi, *Acc. Chem. Res.*, 1997, **30**, 97–102.
- 8 N. C. Blanco, A. Arévalo and J. J. García, *Dalton Trans.*, 2016, **45**, 13604–13614.
- 9 K. Everaere, A. Mortreux and J. F. Carpentier, *Adv. Synth. Catal.*, 2003, **345**, 67–77.
- 10 (a) F. E. Fernández, M. C. Puerta and P. Valerga, *Organometallics*, 2011, **30**, 5793–5802; (b) S. Burling, M. K. Whittlesey and J. M. J. Williams, *Adv. Synth. Catal.*, 2005, **347**, 591–594; (c) Y. Xu, T. Cheng, J. Long, K. Liu, Q. Quian, F. Gao, G. Liu and H. Li, *Adv. Synth. Catal.*, 2012, **354**, 3250–3258.
- 11 (a) L. Yang, A. Krüger, A. Neels and M. Albrecht, *Organometallics*, 2008, **27**, 3161–3171; (b) N. Ding and T. S. Hor, *Dalton Trans.*, 2010, **39**, 10179–10185; (c) S. Semwal, D. Ghorai and J. Choudhury, *Organometallics*, 2014, **33**, 7118–7124.
- 12 P. Melle, Y. Manoharan and M. Albrecht, *Inorg. Chem.*, 2018, **57**, 11761–11774.

- 13 D. Wang, K. Zhao, S. Yang and Y. Ding, *Z. Anorg. Allg. Chem.*, 2015, **641**, 400–404.
- 14 Y. Blum, D. Czarkie, Y. Rahamim and Y. Shvo, *Organometallics*, 1985, **4**, 1459–1461.
- 15 (a) M. Y. Haddad, H. B. Henbest, J. Husbands and T. R. B. Mitchell, *Proc. Chem. Soc., London*, 1964, 361–365; (b) J. Trochagr and H. B. Henbest, *Chem. Commun.*, 1967, 544–544.
- 16 (a) Y. Sasson and J. Blum, *Tetrahedron Lett.*, 1971, **12**, 2167–2170; (b) J. Blum, Y. Sasson and S. Iflah, *Tetrahedron Lett.*, 1972, **13**, 1015–1018; (c) Y. Sasson and J. Blum, *J. Org. Chem.*, 1975, **40**, 1887–1896.
- 17 R. L. Chowdhury and J. E. Bäckvall, *J. Chem. Soc., Chem. Commun.*, 1991, 1063–1064.
- 18 (a) Y. Sun, Y. Guo, Q. Lu, X. Meng, W. Xiaohua, Y. Guo, Y. Wang, X. Liu and Z. Zhang, *Catal. Lett.*, 2005, **100**, 3–4; (b) J. Muzart, *Eur. J. Org. Chem.*, 2015, 5693–5707.
- 19 A. Fujii, S. Hashiguchi, N. Uematsu, T. Ikarita and R. Noyori, *J. Am. Chem. Soc.*, 1996, **118**, 2521–2522.
- 20 S. Ogo, T. Abura and Y. Watanabe, *Organometallics*, 2002, **21**, 2964–2969.
- 21 (a) A. Azua, J. A. Mata and E. Peris, *Organometallics*, 2011, **30**, 5532–5536; (b) O. Prakash, H. Joshi, K. Nayan, P. L. Gupta and A. K. Singh, *Organometallics*, 2014, **33**, 3804–3812.
- 22 (a) M. L. Berch and A. Davison, *J. Inorg. Nucl. Chem.*, 1973, **35**, 3763–3767; (b) R. M. Adkins, R. M. Eloffson, A. G. Rossow and C. C. Robinson, *J. Am. Chem. Soc.*, 1949, **71**, 3622; (c) D. Wang, C. Deraedt, J. Ruiz and D. Astruc, *J. Mol. Catal. A: Chem.*, 2015, **400**, 14–21.
- 23 H. Lundberg and H. Adolfsson, *Synthesis*, 2016, 644–652.
- 24 (a) E. C. Constable, N. Hostettler, C. E. Housecroft, N. S. Murray, J. Schönle, U. Soydaner, R. M. Walliser and J. A. Zampese, *Dalton Trans.*, 2013, **42**, 4970–4977; (b) E. K. V. Beuken, A. Meetsma, H. Kooijman, A. L. Spek and B. L. Feringa, *Inorg. Chim. Acta*, 1997, **264**, 171–183; (c) D. V. Aleksanyan, Y. V. Nelyubina, Z. S. Klemenkova and V. A. Kozlov, *Phosphorus, Sulfur Silicon Relat. Elem.*, 2014, **189**, 1028–1042.
- 25 (a) W. J. Geary, *Coord. Chem. Rev.*, 1971, **7**, 81; (b) K. Nakamoto, *Infrared and Raman Spectra of Inorganic and Coordination Compounds*, Wiley, 1986.
- 26 (a) P. Vijayan, S. Yadav, S. Yadav and R. Gupta, *Inorg. Chim. Acta*, 2020, **502**, 119285; (b) P. Vijayan, P. Viswanathamurthi, P. Sugumar, M. N. Ponnuswamy, M. D. Balakumaran, P. T. Kalaichelvan, K. Velmurugan, R. Nandhakumar and R. J. Butcher, *Inorg. Chem. Front.*, 2015, **2**, 620–639.
- 27 (a) J. Legros, G. Primault, M. Toffano, M. A. Riviere and J. C. Fiand, *Org. Lett.*, 2000, **2**, 433–436; (b) R. Das and M. Kapur, *Asian J. Org. Chem.*, 2018, **7**, 1217–1235; (c) T. Fukushima, D. Ghosh, K. Kobayashi, H. Ohtsu, S. Kitagawa and K. Tanaka, *Inorg. Chem.*, 2016, **55**, 11613–11616; (d) H. Tanaka, B. C. Tzeng, H. Nagao, S. M. Peng and K. Tanaka, *Inorg. Chem.*, 1993, **32**, 1508–1512.
- 28 F. Basuli, S. M. Peng and S. Bhattacharya, *Inorg. Chem.*, 2001, **40**, 1126–1133.
- 29 E. Alessio, G. Mestroni, G. Nardin, W. M. Attia, M. Calligaris, G. Sava and S. Zorzet, *Inorg. Chem.*, 1998, **27**, 4099–4106.
- 30 (a) S. Kumar, R. Kishan, P. Kumar, S. Pachisia and R. Gupta, *Inorg. Chem.*, 2018, **57**, 1693–1697; (b) S. Pachisia and R. Gupta, *Cryst. Growth Des.*, 2019, **19**, 6039–6047.
- 31 D. Bansal, G. Kumar, G. Hundal and R. Gupta, *Dalton Trans.*, 2014, **43**, 14865–14875.
- 32 (a) J. Heinze, *Angew. Chem., Int. Ed. Engl.*, 1984, **23**, 831–847; (b) S. Chakraborty, M. G. Walawalkar and G. K. Lahiri, *J. Chem. Soc., Dalton Trans.*, 2000, 2875–2883.
- 33 A. Mukherjee, A. Nerush, G. Leitus, L. J. W. Shimon, Y. B. David, N. A. E. Jalapa and D. Milstein, *J. Am. Chem. Soc.*, 2016, **138**, 4298–4301.
- 34 (a) J. D. Pasquale, M. Kumar, M. Zeller and E. T. Papish, *Organometallics*, 2013, **32**, 966–979; (b) P. Neta and R. H. Schuler, *J. Am. Chem. Soc.*, 1972, **94**, 1056; (c) C. Battilocchio, J. M. Hawkins and S. V. Ley, *Org. Lett.*, 2013, **15**, 2278–2281; (d) P. Kukula and L. Cerveny, *Res. Chem. Intermed.*, 2000, **26**, 913–922.
- 35 (a) H. Yang, M. A. Gressier, N. Lugan and R. Mathieu, *Organometallics*, 1997, **16**, 1401–1409; (b) S. A. Haut, *J. Agric. Food Chem.*, 1885, **33**, 278–280.
- 36 T. Ohkuma, N. Utsumi, K. Tsutsumi, K. Murata, C. Sandoval and R. Noyori, *J. Am. Chem. Soc.*, 2006, **128**, 8724–8725.
- 37 (a) S. E. Clapham, A. Hadzovic and R. H. Morris, *Coord. Chem. Rev.*, 2004, **248**, 2201–2237; (b) S. Rösler, J. Obenauf and R. Kempe, *J. Am. Chem. Soc.*, 2015, **137**, 7998–8001; (c) A. Flores-Gaspar, P. Pinedo, M. Crestani, M. Muñoz, D. Morales, B. Warsop, W. D. Jones and J. J. Garcia, *J. Mol. Catal. A: Chem.*, 2009, **309**, 1–11; (d) A. Maity, A. Sil and S. K. Patra, *Eur. J. Inorg. Chem.*, 2018, 4063–4073; (e) H. Chai, T. Liu, Q. Wang and Z. Yu, *Organometallics*, 2015, **34**, 5278–5284; (f) W. Du, Q. Wang, L. Wang and Z. Yu, *Organometallics*, 2014, **33**, 974–982.
- 38 J. W. Handgraaf and E. J. Meijer, *J. Am. Chem. Soc.*, 2007, **129**, 3099–3103.
- 39 K. Ganguli, S. Shee, D. Panja and S. Kundu, *Dalton Trans.*, 2019, **48**, 7358–7366.
- 40 S. Bauri, S. N. R. Donthireddy, P. M. Illam and A. Rit, *Inorg. Chem.*, 2018, **57**, 14582–14593.
- 41 Typically, transition metal complexes having the N–H functionality in the resultant [M–H] species/complex follow the outer-sphere mechanism unlike in the present Ru(II) complexes; see M. Perez, S. Elangovan, A. Spannenberg, K. Junge and M. Beller, *ChemSusChem*, 2017, **10**, 83–86 and B. Zhao, Z. Han and K. Ding, *Angew. Chem., Int. Ed.*, 2013, **52**, 4744–4788.
- 42 The binding studies were performed in DMF as the transfer hydrogenation reaction was very fast in 2-propanol that did not allow the observation of any intermediate including [Ru–O<sup>i</sup>Pr].
- 43 D. Bansal and R. Gupta, *Dalton Trans.*, 2016, **45**, 502–507.

- 44 V. Kumar, P. Kumar, S. Kumar, D. Singhal and R. Gupta, *Inorg. Chem.*, 2019, **58**, 10364–10376.
- 45 N. Ghosh, R. Mondal and S. Mukherjee, *Langmuir*, 2015, **31**, 8074–8080.
- 46 The rate constants are considerably lower as the kinetics experiments were performed at room temperature (20 °C) whereas catalytic TH reactions were carried out at 80 °C.
- 47 (a) S. Semwal, I. Mukkatt, R. Thenarukandiyil and J. Choudhury, *Chem. – Eur. J.*, 2017, **23**, 13051–13057; (b) S. Garhwal, B. Maji, S. Semwal and J. Choudhury, *Organometallics*, 2018, **37**, 4720–4725; (c) C. M. Moore, B. Bark and N. K. Szymczak, *ACS Catal.*, 2016, **6**, 1981–1990.
- 48 (a) J. W. Jacobs, J. T. McFarland, I. Wainer, D. Jeanmaier, C. Ham, K. Hamm, M. Wnuk and M. Lam, *Biochemistry*, 1974, **13**, 60–64; (b) K. Bowden and M. Hardy, *Tetrahedron*, 1966, **22**, 1169–1117.
- 49 The time duration for these experiments was 12 h, whereas other catalytic reactions were carried out for 6 h.
- 50 S. Kumar, R. Kishan and R. Gupta, *Indian Patent* 309321, 2019.
- 51 M. L. Berch and A. Davison, *J. Inorg. Nucl. Chem.*, 1973, **35**, 3763–3767.
- 52 D. T. Swayner and J. L. Roberts, *Experimental Electrochemistry for Chemists*, Wiley, New York, 1974.
- 53 N. G. Connelly and W. E. Geiger, *Chem. Rev.*, 1996, **96**, 877.
- 54 *CrysAlisPro*, v. 1.171.33.49b, Oxford Diffraction Ltd., Abingdon, 2009.
- 55 A. Altomare, G. Cascarano, C. Giacovazzo and A. Guagliardi, *J. Appl. Crystallogr.*, 1993, **26**, 343.
- 56 G. M. Sheldrick, *Acta Crystallogr., Sect. A: Fundam. Crystallogr.*, 2008, **64**, 112.
- 57 L. J. Farrugia, *WinGX*, v. 1.70, *An Integrated System of Windows Programs for the Solution, Refinement and Analysis of Single-Crystal X-ray Diffraction Data*, Department of Chemistry, University of Glasgow, 2003.
- 58 (a) S. P. Suna, C. J. Li, J. H. Sunb, S. H. Shi, M. H. Fand and Q. Zhoua, *J. Hazard. Mater.*, 2009, **161**, 1052–1057; (b) M. T. Macpherson, M. J. Pilling and M. J. C. Smith, *J. Phys. Chem.*, 1985, **89**, 2268–2274.
- 59 L. P. Hammett, *J. Am. Chem. Soc.*, 1937, **59**, 96–103.
- 60 C. Hansch, A. Leo and R. W. Taft, *Chem. Rev.*, 1991, **91**, 165–195.